RNA (1999), *5*:646–655. Cambridge University Press. Printed in the USA.

The folding of large RNAs studied by hybridization to arrays of complementary oligonucleotides

MUHAMMAD SOHAIL,[1] SAGHIR AKHTAR,[2] and EDWIN M. SOUTHERN[1]

[1]Department of Biochemistry, University of Oxford, South Parks Road, Oxford, OX1 3QU, England, United Kingdom
[2]Department of Pharmaceutical and Biological Sciences, Aston University, Aston Triangle, Birmingham B4 7ET, England, United Kingdom

ABSTRACT

Folding pathways of large RNAs are poorly understood. We have addressed this question by hybridizing in vitro transcripts, which varied in size, to an array of antisense oligonucleotides. All transcripts included a common sequence and all but one shared the same start-point; the other had a small deletion of the 5′ end. Minimal free energy calculations predicted quite different folds for these transcripts. However, hybridization to the array showed predominant features that were shared by transcripts of all lengths, though some oligonucleotides that hybridized strongly to the short transcripts gave weak interaction with longer transcripts. A full-length RNA fragment that had been denatured by heating and allowed to cool slowly gave the same hybridization result as a shorter transcript. Taken together, these results support theories that RNA folding creates local stable states that are trapped early in the transcription or folding process. As the transcript elongates, interactions are added between regions that are transcribed early and those transcribed late. The method here described helps in identifying regions in the transcripts that take part in long-range interactions.

Keywords: antisense oligonucleotides; mfold; RNA folding; scanning arrays

INTRODUCTION

Secondary folding of an RNA is a major determinant of its higher order conformation and its interaction with a variety of other molecules; it is important to structure–function relationship (Brion & Westhof, 1997). There are two conflicting views on the secondary folding of large RNAs into their final biologically active state. The generally held view is that most secondary interactions in large RNAs are local (e.g., Moras, 1997). It is assumed that local folding is established as the molecule is transcribed, and some early studies showed sequential folding of small RNAs (Boyle et al., 1980; Kramer & Mills, 1981), but there is no similar evidence for large RNAs. The alternative view is that RNAs exist in a global minimal free energy state that would have to be established after synthesis was complete. Though their limitations are well known, researchers tend to use the energy minimization computer programs (e.g., mfold; Zuker, 1989) because they can be easily applied to molecules up to 2–3 kb. Such predictions allow for interactions between distant sequences giving no preference to any local folding that may have occurred during synthesis. While the ability of these programs to predict correct secondary structure of large RNAs is disputed by some (Milner et al., 1997; Schuster et al., 1997; Ho et al., 1998) others believe them to be mostly correct in their predictions (Tinoco & Kieft, 1997).

The uncertainty and difficulty of predicting secondary structure has led to the use of empirical methods to deduce information about complex RNAs. The tertiary structures of several small- and medium-sized RNAs have been resolved to atomic level by X-ray crystallography (Kim et al., 1974; Robertus et al., 1974; Scott et al., 1995; Cate et al., 1996). However, large RNAs (e.g., mRNAs) are difficult to crystallize (Moras, 1997) and thus cannot be analyzed by this method. Approaches to determine secondary structure of RNAs include biochemical and chemical fingerprinting (e.g., Lauber et al., 1997) and phylogenetic analysis of large groups of functional RNAs (Michel & Westhof, 1990). The biochemical and chemical cleavage methods, which identify single- and double-stranded regions, generate limited information and are more suited to small RNAs.

Reprint requests to: Muhammad Sohail, Department of Biochemistry, University of Oxford, South Parks Road, Oxford, OX1 3QU, England, United Kingdom; e-mail: msohail@bioch.ox.ac.uk.

The phylogenetic approach, which assumes that sequences with similar biological function acquire homologous secondary structure has proved to be the most successful among predictive methods for deriving RNA secondary structure. However, it cannot be applied when the number of sequences is small and is unlikely to be useful if the folded structure has no functional significance, as is likely to be the case for most mRNAs. Therefore, there is a constant need to develop new approaches to analyze the structure of large RNAs at all levels.

We describe an analysis of the folding pathway of an mRNA by hybridizing transcripts of increasing length to an array of complementary oligonucleotides, which suggests that much of the local folding established early in transcription persists, but is detectably modified by interactions with regions transcribed later.

RESULTS

Hybridization of transcripts of various lengths to the scanning array

To obtain transcripts of various sizes, the plasmid pGEMB5 DNA was digested with appropriate restriction endonucleases to produce templates terminating at four different positions at 3′-end for use in transcription. Transcriptions were carried out under the control of a T7 promoter in the presence of a radiolabeled precursor (Fig. 1). These transcripts were used in hybridization to a scanning array of antisense oligonucleotides.

The scanning array, ranging in size from monomers to 21-mers, represented complements of 111 nt (including positions 114–224) located within the mRNA for cyclin B5 (Figs. 1 and 3). The organization and structure of the scanning array are described in Figure 2. The longest oligonucleotides were made along the center line of the array, which represented a 21-nt sliding window of oligonucleotides complementary to the transcripts; the tips of the large diamond shapes were occupied by mononucleotides. In between were cells containing all lengths between 1 and 21. For each length of oligonucleotides, s, there are $N - s + 1$ s-mers covering a total target length of N bases. Therefore, there are 111 monomers and 91 21-mers. The array as synthesized is symmetrical above and below the center line of the template and each oligonucleotide is represented twice allowing for duplicate measurements of hybridization levels.

The patterns of hybridization to the array shared common features

The 175-nt transcript (which terminates at position 175 on the array) showed significant hybridization to oligonucleotides in areas a, b and d (Fig. 3). Some hybridization was also shown with the oligonucleotides at the position marked with an open triangle, which only has part of its complement in the 175-nt transcript (sequence given in the corresponding histogram panel).

The 336-nt fragment, which covered the whole of the array, was the transcript which showed most regions of hybridization; an additional hybridization area, c in Figure 3, was shown that was not represented in the 175-nt transcript. Some oligonucleotides in area a showed weaker hybridization and some in area b stronger as compared with the 175-nt transcript. The oligonucleotides at the open triangle position also showed stronger hybridization with the 336-nt transcript, probably because its full complement was present in this transcript.

Further extension of the transcription products to 512 nt and 1,389 nt produced hybridizations that were very similar to each other, but did not show any additional hybridization above the 336-nt transcript. Indeed, certain features seen in hybridization with shorter transcripts were lost. For example, there was no hybridiza-

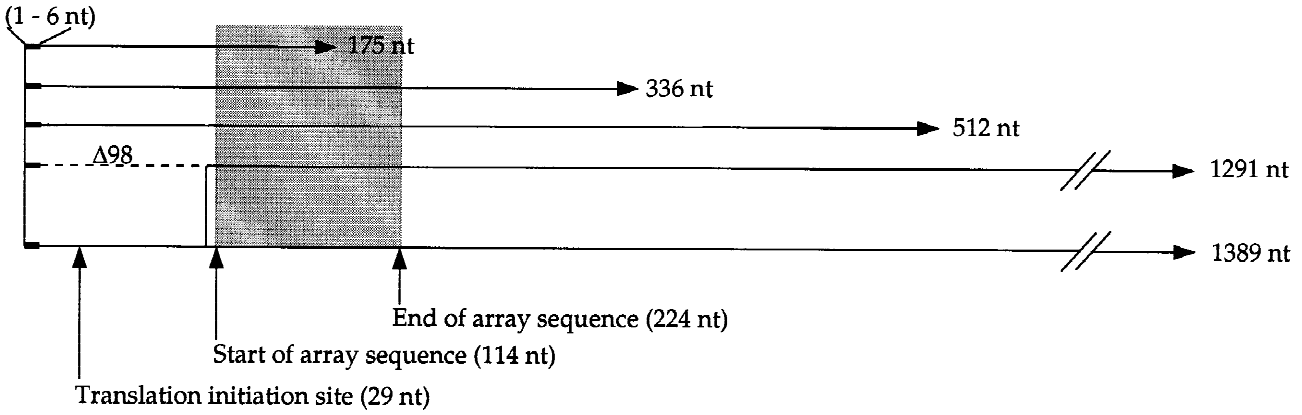

FIGURE 1. The origins of the various transcripts are shown. Transcriptions were under the control of a T7 promotor and all transcripts have the first 6 nt from the T7 promotor sequence (5′ ggg aga) and the numbers are inclusive of those. Translation initiation site and sites of array sequence start and end are also labeled.

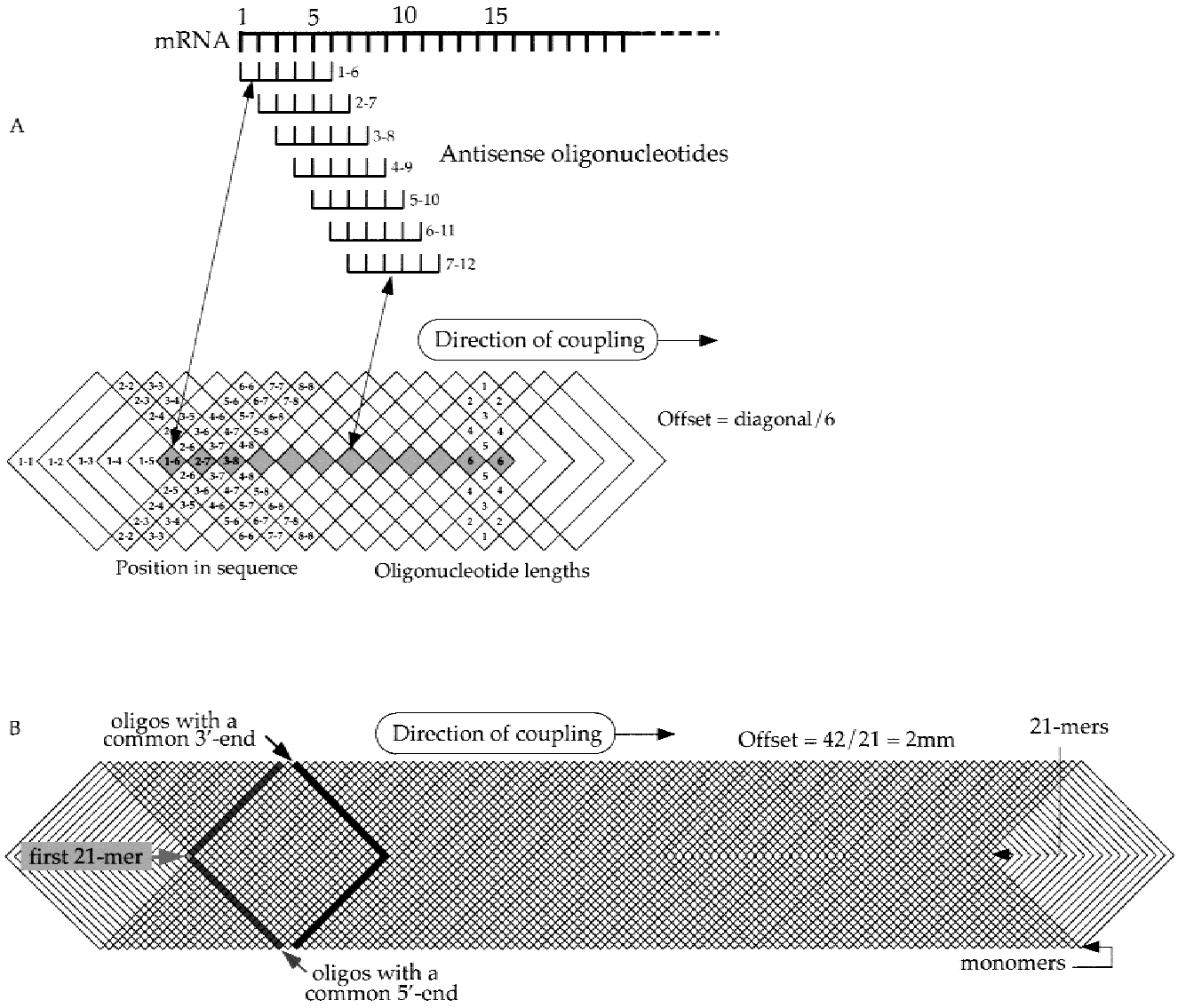

FIGURE 2. Organization of a scanning array. **A**: a template of overlapping diamonds representing the footprints of a diamond-shaped mask used to make a scanning array. The tiling path on the top shows the positions of some of the longest oligonucleotides (located along the center line) in the grid. A cell is created by pressing a diamond-shaped mask against the polypropylene substrate. Synthesis is carried out on an automated DNA synthesizer, such as ABI 394. DNA synthesis reagents are introduced at the bottom of the cell and removed from the top or the bottom. With the use of standard nucleotide phosphoramidites in synthesis, the oligonucleotides are attached to the solid support at their 3′-ends. After each coupling step, the mask is moved along the substrate by a predetermined step size (offset). At each step, the length of the oligonucleotides is the number of bases that have been coupled at the point where the back of the mask passes the front. The first longest oligonucleotide on the array is made after the number of coupling steps which equal "diagonal of the mask/step size." Thus for a mask with a diagonal of 42 mm and coupling step size of 2 mm, the first 21-mer would be synthesized at step number 21. Before this are all lengths from mononucleotide to 20-mer. **B**: A template of overlapping diamonds generated by the computer program, xvseq, that was used to analyze the images obtained after hybridization shown in Figure 3. Drawings are not to scale.

tion in area d in Figure 3; several oligonucleotides in areas a, b and c showed much weaker hybridization.

The 175-nt transcript also hybridized to oligonucleotides on the array the complements of which were not present in the transcript (Fig. 3, marked with a closed triangle). It is noticeable that shorter oligonucleotides gave greater duplex yield than the 21-mer in this case. The shortest oligonucleotide showing detectable hybridization was a hexamer [5′ ccactt] and the oligonucleotide showing maximum hybridization was a decamer [5′ ccactttctg] (data not shown). Neither the hexamer nor the decamer has a fully complementary counterpart in the 175-nt transcript.

A 1,291-nt transcript (Δ98) with 98 nt of the 1,389-nt transcript deleted at the 5′ end showed no significant difference from the other long transcripts except for

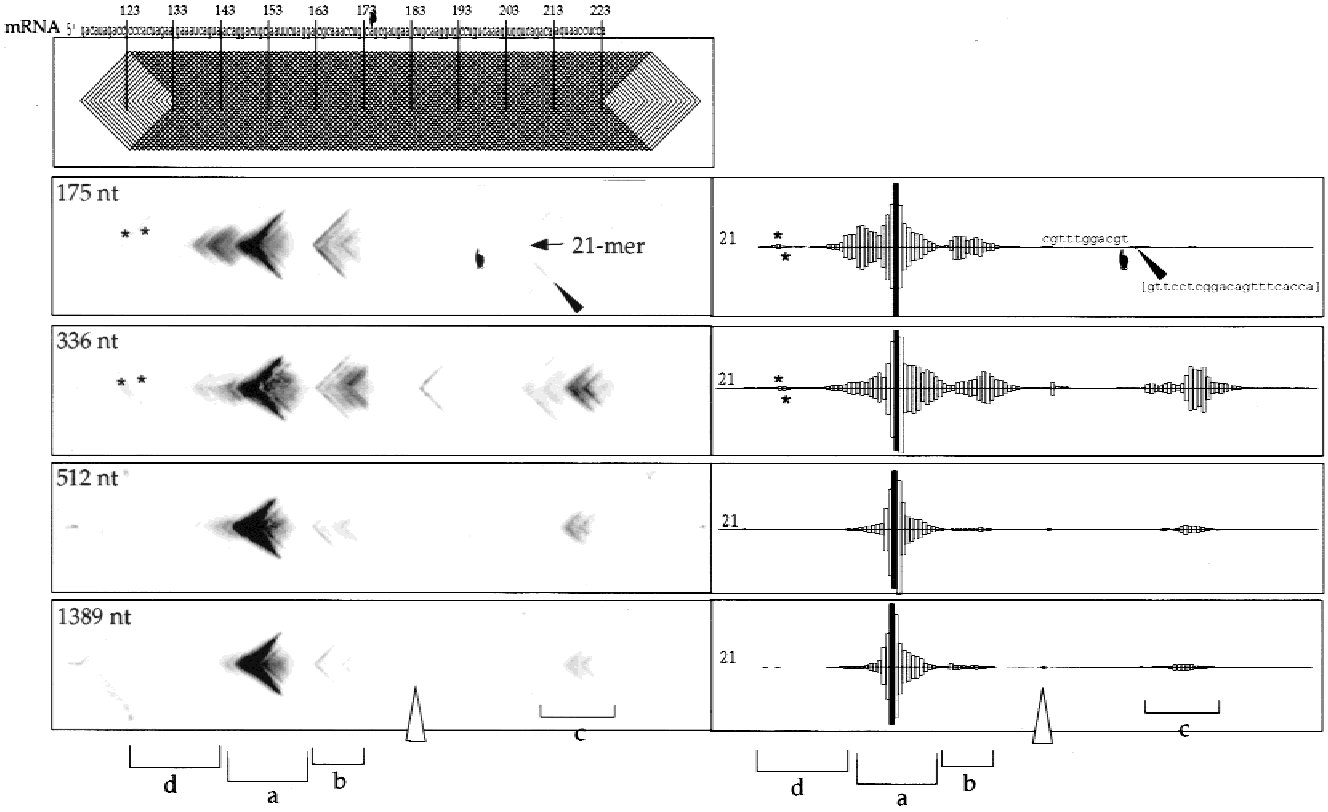

FIGURE 3. Hybridization of the mRNA fragments of various sizes with a common 5′ end to an array of complementary oligonucleotides scanning a 111-nt sequence. The series of diamond-shaped templates used to analyze the images is shown in at the top. The tips of the large diamond shapes are occupied by mononucleotides; the longest oligonucleotides are in the row of cells running along the center line. Every tenth position is marked with a vertical line across the mRNA sequence into the template. The images obtained after hybridization (left) were analyzed using xvseq (Elder et al., 1999). A template comprising a series of 111 overlapping diamonds (top; also see Fig. 2) was placed over the images to generate cells containing individual oligonucleotide sequences. Each region within the cells of the images was integrated. The histograms (right) present the integrated pixel values for the areas on the array carrying 21-mers and the two values for the areas above and below the center line of the array. Three major areas of hybridization are marked a, b, and c. The oligonucleotides marked with asterisks hybridized only when 175-nt and 336-nt transcripts were used. The 175-nt transcript terminates at the marked (☛) position and has a complement of only an 11-mer at the position marked with an open triangle. The sequence given in brackets in the 175-nt histograms does not have its complement in the 175-nt transcript. It is also noticeable that the duplex yield is greater for shorter oligonucleotides (situated towards the ends of the chevron) compared with the 21-mer at this position. Some hybridizations are not visible in the images (for example, in region c of 512-nt and 1,389-nt hybridizations) but they can be identified in the histograms.

differences in the relative duplex yields (Fig. 4). Most notably, area d, which hybridizes to the 175-nt and 336-nt but not to the 512-nt and 1,389-nt transcripts, also hybridized to Δ98.

Hybridization of a denatured/renatured transcript to the array

A full length transcript that had been denatured by heating and allowed to renature by slow cooling showed a pattern of hybridization strikingly similar to that of the 336-nt transcript (Fig. 4). Gel electrophoresis of the annealed RNA showed that it had not been reduced in size by heat treatment. The oligonucleotides labeled with asterisks are those seen in hybridizations with the 336-nt and 175-nt transcripts.

Mfold-predicted structures of the transcripts

Mfold predictions of the structures of transcripts used in this study (Fig. 5) showed different overall secondary conformations for RNAs of the various sizes. In particular, regions analyzed on the array showed quite different predicted folds. For example, region a is different in 1,389-nt fold compared with the 512-nt fold but similar to that in 175-nt structure. Region b is different in all cases. Similar variations could be seen in other parts of the predicted structures.

DISCUSSION

There is compelling evidence that duplex formation between oligonucleotides and long nucleic acids is constrained by the secondary folding of the RNA and

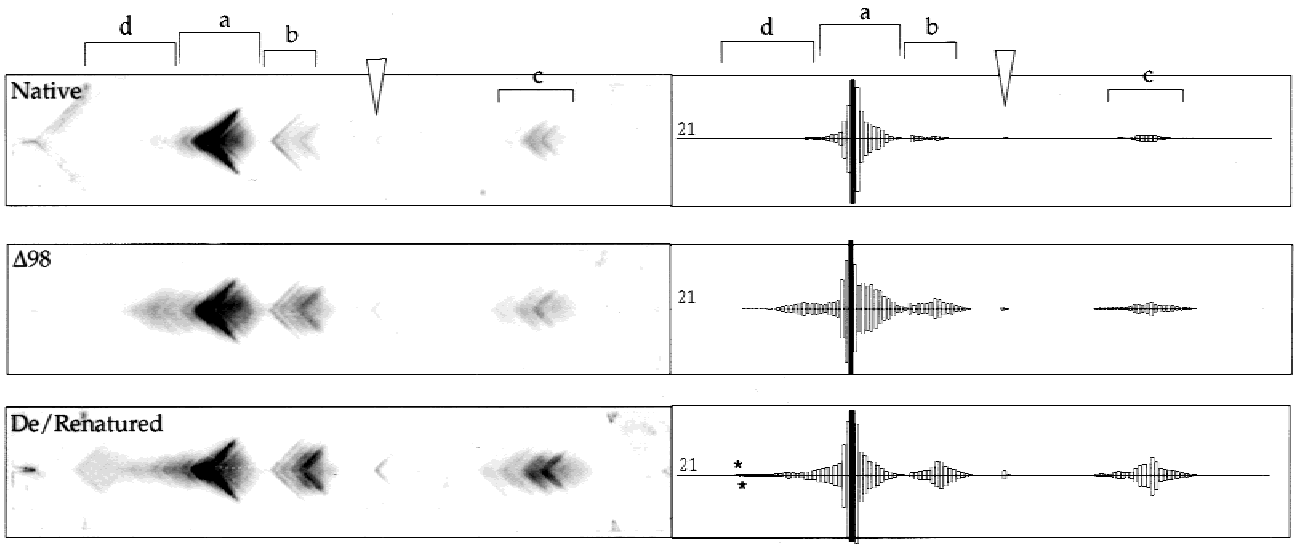

FIGURE 4. The top panel shows hybridization of the native 1,389-nt transcript. The middle panel shows hybridization of the 1,389-nt denatured/renatured transcript. In this experiment the transcript was heated to 85 °C for 5 min to denature and then allowed to cool slowly (at 6 °C/min) to 22 °C. and then used in hybridization. The lower panel shows hybridization of the 1,291-nt transcript in which 98 nt of the full length RNA are deleted at the 5′ end. The analysis of the arrays was carried out as described in Figure 2.

is not determined primarily by base composition or sequence (Southern et al., 1994; Frauendorf & Engels, 1996; Toulme et al., 1996; Milner et al., 1997; Ho et al., 1998). The effects of thermodynamic and kinetic factors on folding and stabilities of the folded structures are also not well understood (Konings & Gutell, 1995). The experiments reported here give a comparison of the global minimal free energy structures of RNAs with their hybridization behavior to complementary oligonucleotides. Several pieces of evidence showed that local folding established early in transcription largely persists and that possibly large RNA molecules do not reach a global free energy minimal structure.

The 175-nt transcript, the shortest in the set, represents an early stage of transcription. The folds already established in this transcript determine the strongest features of the hybridization pattern. The similarity of the hybridization patterns suggests that the structural components established early in transcription were carried over in the longer transcripts. For example, striking pattern of hybridization in region a is seen for all transcripts. If the pattern is determined by the RNA fold, then this fold must be retained in the longer transcripts.

Several oligonucleotides showed higher duplex yields with smaller transcripts than with longer. Such differences in relative duplex yield are likely to be a result of steric constraints that are more prominent in the longer RNA molecules than in shorter. In longer molecules sites accessible to duplex formation may be masked by the three-dimensional folding of the molecules and also by additional tertiary interactions; accessibility is increased in shorter transcripts where these interactions are absent. As RNA synthesis proceeds, secondary interactions start to establish making some sequences accessible but not the others. With the further elongation of the chain, however, more structures are added which mask the accessible sites made already, thus reducing the extent of heteroduplex formation.

Two pieces of evidence suggest that there is an interaction between sequences in region d and the region between 336 and 512. First, oligonucleotides in this area showed hybridization to the 175-nt and 336-nt transcripts and not to the 512-nt transcript. This implies that this region of mRNA interacts with the 5′ end and thus masks the accessibility of oligonucleotides in area d (not predicted in the mfold). Second, a deletion in the 5′ end (Δ98) also makes the oligonucleotides in area d accessible to hybridization, albeit more weakly than the shortest transcript. It is also noticeable that some oligonucleotides in area a located closer to d are most strongly hybridized in the 175-nt transcript hybridization. Since the evidence suggests an interaction between d and the 336–512 region, it is possible that the 98-nt deletion destabilizes this interaction, making the oligonucleotides more accessible. In the case of the 175-nt transcript, this interaction is absent altogether, resulting in a much stronger hybridization.

The data on denatured/renatured RNA suggest that the fold is close to that of the native transcript (i.e., the structure before melting), but some structural features present in the native appear to be absent from the refolded molecule. The increase in the accessibility of some oligonucleotides in region d (marked with as-

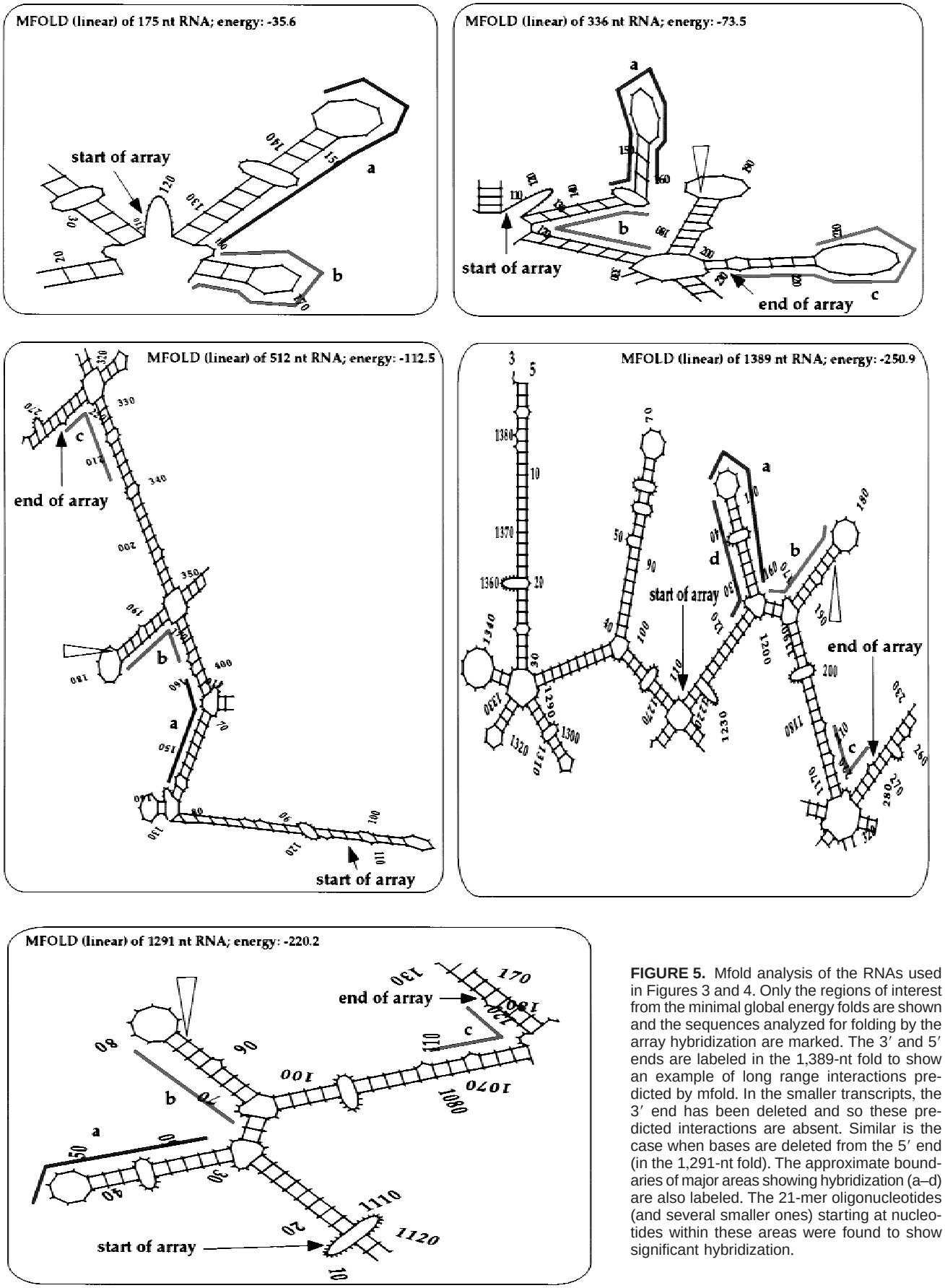

FIGURE 5. Mfold analysis of the RNAs used in Figures 3 and 4. Only the regions of interest from the minimal global energy folds are shown and the sequences analyzed for folding by the array hybridization are marked. The 3′ and 5′ ends are labeled in the 1,389-nt fold to show an example of long range interactions predicted by mfold. In the smaller transcripts, the 3′ end has been deleted and so these predicted interactions are absent. Similar is the case when bases are deleted from the 5′ end (in the 1,291-nt fold). The approximate boundaries of major areas showing hybridization (a–d) are also labeled. The 21-mer oligonucleotides (and several smaller ones) starting at nucleotides within these areas were found to show significant hybridization.

terisks), which is most likely to interact with a distant region between nucleotide positions 336 and 512, indicates that their native interaction failed to reestablish during renaturation. It is thus likely that short-range interactions are established first before procession to distant interactions (also see Zarrinker & Williamson, 1994; Batey & Doudna, 1998).

The 175-nt transcript hybridized to oligonucleotides whose complement was absent from the transcript. Although, it is not possible to predict which duplexes result from Watson–Crick pairing, this particular hybridization is more likely to have resulted from a non-Watson–Crick interaction between RNA and the antisense oligonucleotides. Another example of a shorter sequence (a dinucleotide, gg) producing stronger hybridization to a complementary target than many fully complementary oligonucleotides has also been reported (Southern et al., 1994). These types of interactions can be a problem in methods which rely on sequence-specific hybridization (e.g., Wodicka et al., 1997; Drmanac et al., 1998; de Saizieu et al., 1998). Several procedures that involve the use of fragmented RNA (e.g., for transcript imaging: Wodicka et al., 1997; de Saizieu et al., 1998) can also produce nonspecific heteroduplexes. Such interactions appear to be rare (only one example could be detected in this study) and difficult to identify in these protocols; the data thus obtained must be analyzed with caution.

Mfold predicted structures and implication of the hybridization results

The large differences seen in the mfold-predicted structures would be expected to have profound effects on the accessibility to duplex formation by oligonucleotides and lead to qualitatively different patterns rather than the variation in duplex yield observed.

Several thermodynamic-based methods were devised in the 1980s to predict the secondary structure of RNAs (e.g., Nussinov & Jacobson, 1980; Dumas & Ninio, 1982) and were improved subsequently. These methods were mostly based on the known structure of tRNAs and thermodynamic studies of small RNA fragments in solution (e.g., Tinoco et al., 1973). tRNAs are comparatively small and probably exist in the minimal global free energy state and so their secondary structure can be accurately predicted by computational methods. The algorithms devised by Zuker and colleagues (e.g., Zuker, 1989) became widely used (e.g., mfold) because of their ability to calculate the free energy of folds of longer sequences.

For long RNA molecules, energy calculations often return a number of different structures with similar free energies: there is difficulty in choosing the correct one. We analyzed the full length B5 transcript to see if the free energy of the most stable fold differed significantly from that of the fold in which the 5′ end was constrained to its most stable fold. The minimum free energy of the full transcript was −250.9 kcal/mol and the sum of the free energies of the two parts folded separately was −248.2 kcal/mol, showing that there was little difference between them. This result reemphasizes the problem of using global free energy calculations. Our results further indicate that the predicted structures have limited usage in biological application such as designing antisense oligonucleotides. Ho et al. (1998) have also shown that accessible sites cannot be mapped on predicted structures and that there is no obvious structural difference between accessible and inaccessible regions on the computer folded structures. Gaspin & Westhof (1995) have devised an approach according to the RNA hierarchical folding view that allows for the dynamic incorporation of folding constraints, enabling the user to participate in the computational folding of RNA. They predicted the secondary structure of Group I intron *Td* and RNAseP of *Escherichia coli* with this method, and the results were similar to those predicted by phylogenetic comparison. Despite its demonstrated usefulness, such an approach requires substantial experimental data for input that may not be available for some biological applications, in which case empirical approaches become more useful.

Our results suggest ways in which hybridization to arrays may be used in predicting the secondary interactions in RNA molecules. First, the hybridization data can help in testing short range interactions. Studies of tRNA (K.U. Mir & E.M. Southern, submitted) suggest that strong interactions of oligonucleotides with the target, which are easily identified on the arrays, indicate certain stem-loop structures, and may point to stack interfaces. The 5′ regions of B5 mRNA that hybridize strongly to oligonucleotides, shown against the predicted secondary structure of lowest free energy (Fig. 6), conform with the partial rules derived from the analysis of tRNA. Second, long-range interactions are indicated by the loss of hybridization that results from extending the transcript. The sequences of the oligonucleotides whose hybridization is blocked by the secondary interactions can be read directly from the array to locate the interacting regions precisely.

Analysis of the shortest sequences within the 21-mers showing detectable hybridization revealed that in most cases the optimal binding was achieved by sequences shorter than 21 nt. Further addition of bases (at 3′ end) produced only a small increase in their binding, as indicated by the hybridization intensity values. For example in the case of the 21-mer oligonucleotide 1, optimal binding was achieved by a 14-mer and further addition of bases at its 3′ end produced only a small increase in its binding affinity. It is striking that several oligonucleotides showing optimal hybridization within each area (a, b, or c) terminate at a common base at their 3′ end (e.g., 1 and 2 and 3, 4, and 5).

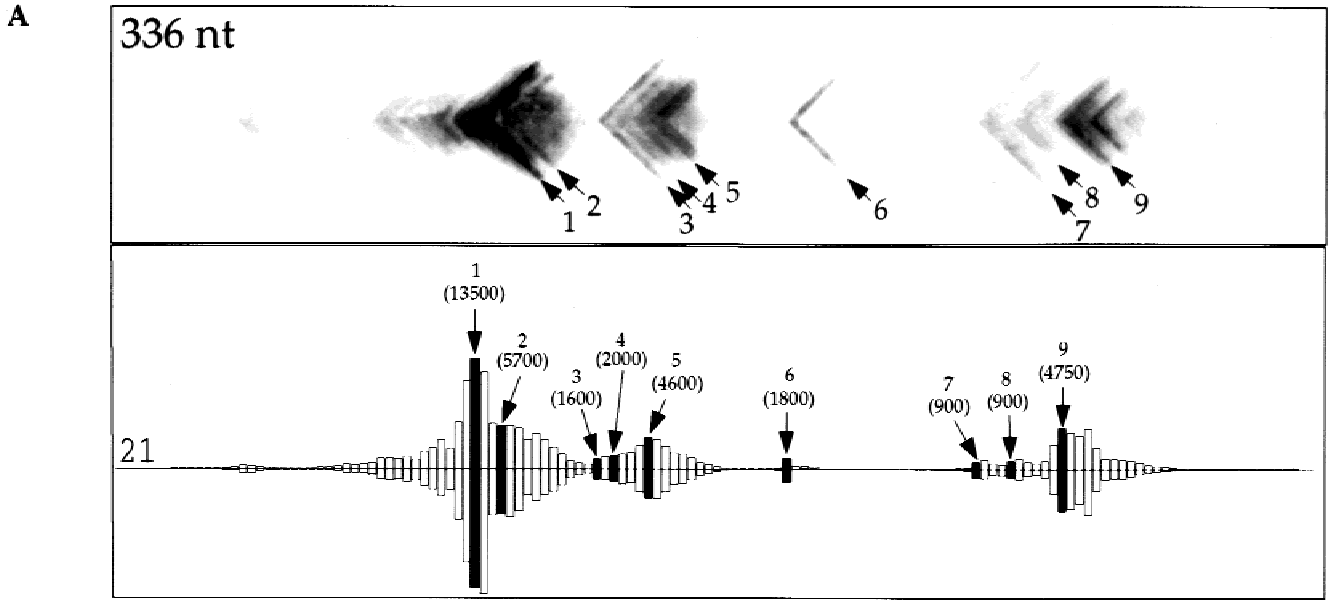

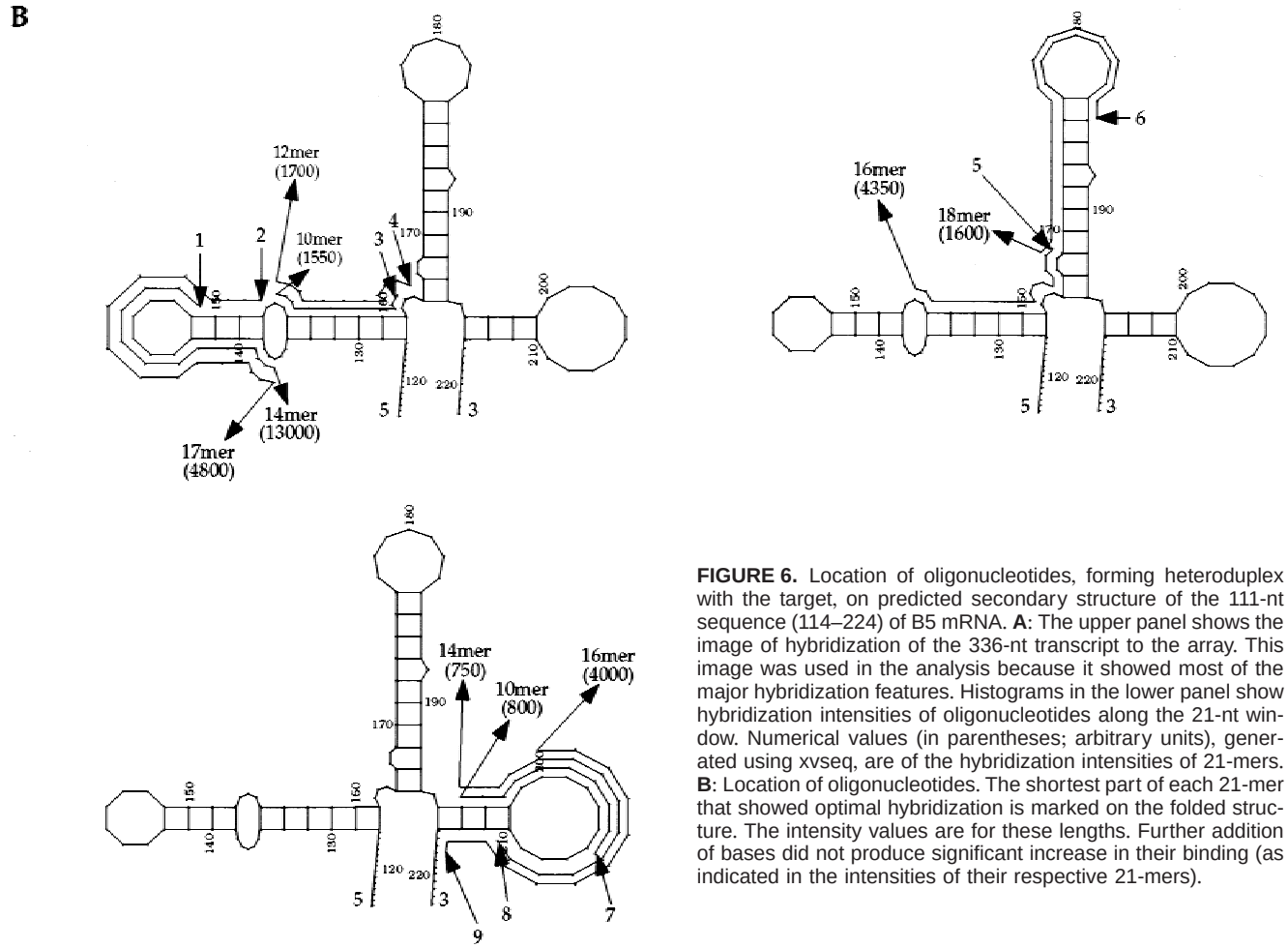

FIGURE 6. Location of oligonucleotides, forming heteroduplex with the target, on predicted secondary structure of the 111-nt sequence (114–224) of B5 mRNA. **A**: The upper panel shows the image of hybridization of the 336-nt transcript to the array. This image was used in the analysis because it showed most of the major hybridization features. Histograms in the lower panel show hybridization intensities of oligonucleotides along the 21-nt window. Numerical values (in parentheses; arbitrary units), generated using xvseq, are of the hybridization intensities of 21-mers. **B**: Location of oligonucleotides. The shortest part of each 21-mer that showed optimal hybridization is marked on the folded structure. The intensity values are for these lengths. Further addition of bases did not produce significant increase in their binding (as indicated in the intensities of their respective 21-mers).

MATERIALS AND METHODS

Synthesis of primers and DNA amplification

PCR primers were synthesized on an Applied Biosystem's 392 DNA/RNA synthesizer. The primers D98 (5′ taatacgactcac tatagggagaaagtacatggacatagacc) and 3END (5′ cccgggcgag ctcggaa) were used on the plasmid pGEMB5 (carrying gene for *Xenopus laevis* Cyclin B5; a gift from Dr. Tim Hunt) to obtain a PCR product with a deletion of 98 bp at the 5′ end of the full-length template for use in in vitro transcription. DNA amplification was carried out in a PTC-200 DNA Engine (MJ Research) using 30 cycles of 94 °C for 1 min, 59 °C for 1 min and 73 °C for 2 min with a final extension step of 10 min at 73 °C. Amplitaq DNA polymerase (Perkin-Elmer) with the recommended buffer was used in amplification. The reactions were purified using Qiagen PCR Purification Kit (Qiagen) according to the manufacturer's instructions.

Preparation of labeled RNA transcripts

Plasmid pGEMB5 was used to obtain full length B5 transcripts and was digested with restriction endonucleases at appropriate sites to obtain DNA templates for use in transcription to obtain transcripts of 175-nt, 336-nt, 512-nt, and 1,389-nt lengths. A transcript with a 98-nt deletion at the 5′ end was obtained from the PCR product obtained with primers D98 (which has the T7 promotor at its 5′ end) and 3END. In vitro transcriptions were carried out with T7 RNA polymerase (Promega) using standard protocol in the presence of [α-^{32}P] UTP (Amersham; 3,000 Ci/mmol). The reactions were at 30 °C for 90 min and desalted by Sephadex-G25 (Pharmacia) column chromatography. Transcripts were analyzed on a 5% denaturing polyacrylamide gel.

Fabrication of arrays

The oligonucleotide array (complement of 111 nt including positions 114–224 in the Cyclin B5 mRNA) was prepared directly onto the surface of aminated polypropylene (Matson et al., 1994) on an adapted Applied Biosystem's DNA synthesizer (ABI 381 A) using a 42-mm diamond-shaped mask as described previously (Southern et al., 1994). Standard phosphoramidites were used in the synthesis. The offset between each coupling step was 2 mm and thus the longest oligonucleotides produced were 21-mers. The arrays were deprotected in 30% ammonia solution at 55 °C for 16 h in a closed chamber (Southern et al., 1994).

Hybridization conditions and analysis

Hybridizations were performed in 1 M NaCl in the the presence of 10 mM Tris, pH 7.4, 1 mM EDTA, and 0.01% SDS at 22 °C for 3 h. Approximately, 50–60 fmol of the transcript was diluted in 12 mL hybridization solution and hybridizations were carried out in a rolling hybridization chamber at 3–4 rpm. The array was then washed in the hybridization solution briefly and dried in layers of Wattman paper. Autoradiography and analysis were carried out essentially as described in Elder et al. (1999). The array was stripped in 100 mM sodium carbonate/bicarbonate buffer (pH 10) containing 0.01% SDS for 2–3 min at 90–95 °C and reused.

Minimal free energy folding of mRNAs

The minimal free energy structures of mRNAs were predicted using the program mfold (Genetics Computer Group, Madison, WI) according to Zuker's latest energy minimization calculations, which are provided on the University of Oxford Molecular Biology Data Center UNIX. The results were printed as "squiggles" output.

ACKNOWLEDGMENTS

The authors thank Tim Hunt, Helfrid Hochegger, Andrea Klotzbücher and Réné Le Guelle for providing the sequence of cyclin B5 and the plasmid pGEMB5.

Received December 16, 1998; returned for revision January 20, 1999; revised manuscript received February 24, 1999

REFERENCES

Batey RT, Doudna JA. 1998. The parallel universe of RNA folding. *Nature Struct Biol 5*:337–340.

Boyle J, Robillard GT, Kim SH. 1980. Sequential folding of transfer RNA: A nuclear magnetic resonance study of successively longer tRNA fragments with a common 5′ end. *J Mol Biol 139*:601–625.

Brion P, Westhof E. 1997. Hierarchy and dynamics of RNA folding. *Annu Rev Biophys Biomol Struct 26*:113–137.

Cate JH, Gooding AR, Podell E, Zhou K, Golden BL, Kundrot CE, Cech TR, Doudna JA. 1996. Crystal structure of a Group I ribozyme domain: Principles of RNA packing. *Science 273*:1678–1685.

de Saizieu A, Certa U, Warrington J, Gray C, Keck W, Mous J. 1998. Bacterial transcript imaging by hybridization of total RNA to oligonucleotide arrays. *Nature Biotech 16*:45–48.

Drmanac S, Kita D, Labat I, Brian H, Schmidt C, Burczak JD, Drmanac R. 1998. Accurate sequencing by hybridization for DNA diagnostics and individual genomics. *Nature Biotech 16*:54–58.

Dumas J-P, Ninio J. 1982. Efficient algorithms for folding and comparing nucleic acid sequences. *Nucleic Acids Res 10*:197–206.

Elder KJ, Johnson M, Milner N, Mir KU, Sohail M, Southern EM. 1999. Antisense oligonucleotide scanning arrays. In: Schena M, ed. *DNA microarrays: A practical approach*. Oxford, United Kingdom: IRL Press. In press.

Frauendorf A, Engels JW. 1996. Interaction of linear and folded modified antisense oligonucleotides with sequences containing secondary structure elements. *Bioorg Med Chem Lett 4*:1019–1024.

Gaspin C, Westhof E. 1995. An interactive framework for RNA secondary structure prediction with a dynamical treatment of constraints. *J Mol Biol 254*:163–174.

Ho SP, Bao Y, Lesher T, Malhotra R, Ma LY, Fluharty SJ, Sakai RR. 1998. Mapping of RNA accessible sites for antisense experiments with oligonucleotide libraries. *Nature Biotech 16*:59–63.

Kim SH, Suddath FL, Quigley GJ, McPherson A, Sussman JL, Wang AJH, Seeman NC, Rich A. 1974. Three-dimensional tertiary structure of yeast phenylalanine transfer RNA. *Science 185*:435–440.

Konings DAM, Gutell RR. 1995. A comparison of thermodynamic foldings with comparatively derived structures of 16S and 16S-like rRNAs. *RNA 1*:559–574.

Kramer FR, Mills DR. 1981. Secondary structure formation during RNA synthesis. *Nucleic Acids Res 9*:5109–5124.

Lauber E, Guilley H, Richards K, Jonard G, Gilmer D. 1997. Conformation of the 3′-end of the beet necrotic yellow vein benevirus RNA 3 analyzed by chemical and enzymatic probing and mutagenesis. *Nucleic Acids Res* 25:4723–4729.

Matson RS, Rampal JB, Coassin PJ. 1994. Biopolymer synthesis on polypropylene supports. I. Oligonucleotides. *Anal Biochem 217*: 306–310.
Michel F, Westhof E. 1990. Modelling of the three-dimensional architecture of Group I catalytic introns based on comparative sequence analysis. *J Mol Biol 216*:585–610.
Milner N, Mir KU, Southern EM. 1997. Selecting effective antisense reagents on combinatorial oligonucleotide arrays. *Nature Biotech 15*:537–541.
Moras D. 1997. A major leap towards the tertiary structure of large RNAs. *RNA 3*:111–113.
Nussinov R, Jacobson AB. 1980. Fast algorithm for predicting the secondary structure of single-stranded RNA. *Proc Natl Acad Sci USA 77*:6309–6313.
Robertus JD, Lander JE, Finch JT, Rhodes D, Brown RS, Clark BFC, Klug A. 1974. Structure of yeast phenylalanine tRNA at 3 Å resolution. *Nature 250*:546–551.
Schuster P, Stadler PF, Renner A. 1997. RNA structure and folding: From conventional to new issues in structure predictions. *Curr Opin Struct Biol 7*:229–235.
Scott WG, Finch JT, Klug A. 1995. The crystal structure of an all-RNA hammerhead ribozyme: A proposed mechanism for RNA catalytic cleavage. *Cell 81*:991–1002.
Southern EM, Case-Green SC, Elder JK, Johnson M, Mir KU, Wang L, Williams JC. 1994. Arrays of complementary oligonucleotides for analyzing the hybridization behavior of nucleic acids. *Nucleic Acids Res 22*:1368–1373.
Tinoco I, Borer PN, Dengler B, Levine MD, Uhlenbeck OC, Crothers DM, Gralla J. 1973. Improved estimation of secondary structure in ribonucleic acids. *Nature New Biol 246*:40–41.
Tinoco I, Kieft JS. 1997. The ion core in RNA folding. *Nature Struct Biol 4*:509–512.
Toulme JJ, Le Tinevez R, Brossalina E. 1996. Targeting RNA structure by antisense oligonucleotides. *Biochimie 78*:663–673.
Wodicka L, Dong H, Mittmann M, Ho M-H, Lockhart DJ. 1997. Genome-wide expression monitoring in *Saccharomyces cerevisiae*. *Nature Biotech 15*:1359–1367.
Zarrinker PP, Williamson JR. 1994. Kinetic intermediates in RNA folding. *Science 265*:918–924.
Zuker M. 1989. On finding all suboptimal foldings of an RNA molecule. *Science 244*:48–52.